Reactive Template-Induced Self-Assembly to Ordered Mesoporous Polymeric and Carbonaceous Materials

Yeru Liang, Ruowen Fu, and Dingcai Wu*

Materials Science Institute, PCFM Lab and DSAPM Lab, School of Chemistry and Chemical Engineering, Sun Yat-sen University, Guangzhou 510275, P. R. China

ABSTRACT As an important method for preparing ordered mesoporous polymeric and carbonaceous materials, the organic template directed self-assembly is facing challenges because of the weak noncovalent interactions between the organic templates and the building blocks. Herein we develop a novel reactive template-induced self-assembly procedure for fabrication of ordered mesoporous polymer and carbon materials. In our approach, the aldehyde end-group of reactive F127 template can react with the resol building block to *in-situ* form a stable covalent bond during the self-assembly process. This is essential for an enhanced interaction between the resol and the template, thus leading to the formation of an ordered body-centered cubic mesostructure. We also show that the ordered mesoporous carbon product exhibits superior capacitive performance, presenting an attractive potential candidate for high performance supercapacitor electrodes.

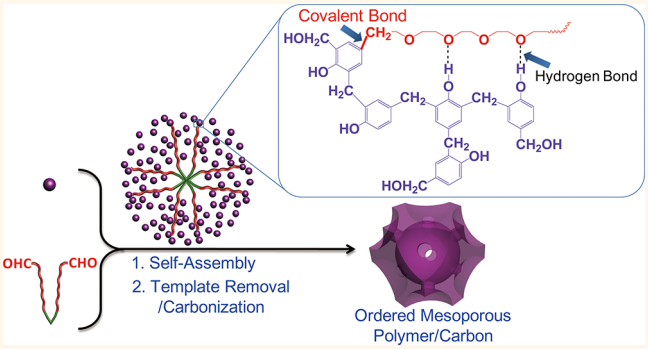

KEYWORDS: reactive template-induced self-assembly · covalent interaction · ordered body-centered cubic mesostructure · porous polymer and carbon · supercapacitor

Construction of well-defined porous materials has always been one of the most active areas in materials science, not only for their fundamental scientific interest, but also for many modern-day technological applications.[1−14] Significant progress has been attained in structural, compositional, and topological control in both inorganic and organic nanoporous structured materials. In recent years, there has been a growing focus on the synthesis and examination of porous materials with ordered mesopore array owing to their unique characteristics including highly periodic pore arrangement, uniform mesopore size, high surface area, and large pore volume.[15−23] These features are of great interest for a broad spectrum of applications, including energy storage, absorption, separation, drug delivery and catalysis.[24−31]

In general, organic template-directed self-assembly is one of the most promising approaches toward synthesis of ordered mesoporous polymeric and carbonaceous materials.[32−36] Those organic compounds like amphiphilic surfactants and block copolymers, which can self-organize into a diversity of supermolecular structures, are generally used as pore templates. Cooperative self-assembly can drive building blocks around the supermolecular structures to form a well-defined organic−organic mesophase. Direct removal of the organic templates by calcination or extraction with solvents leads to mesoporous framework. This organic template pathway has offered a powerful route to fabrication of ordered mesoporous polymer (OMP) and carbon (OMC) materials with various mesostructures, suitable shapes, and designed functionalities. Despite these developments, however, challenges still remain, considering that in most cases, these ordered mesoporous products are not easily obtained by using the common organic template synthetic techniques. The main reason could be ascribed to the fact that organic templates usually interact with building blocks through noncovalent interactions such as hydrogen bonding, van der Waals forces, and electrostatic interaction, which could be too weak to act as a driving force for formation of ordered mesostructures.[32,37]

* Address correspondence to wudc@mail.sysu.edu.cn.

Received for review December 18, 2012 and accepted January 22, 2013.

Published online January 22, 2013
10.1021/nn305841e

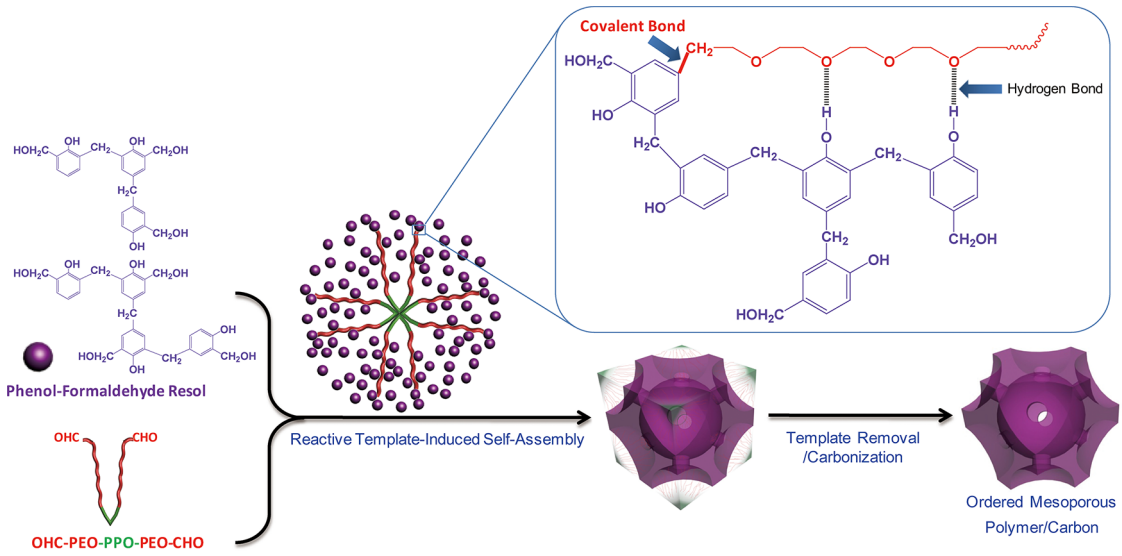

Figure 1. Schematic diagram for the route of reactive template-induced self-assembly to prepare the ordered mesoporous polymer and carbon materials.

In this report, we describe a new strategy to address this shortcoming, which is based on the *in-situ* formation of strong covalent interactions during self-assembly. A reactive template is designed and introduced to induce a self-assembly with phenol-formaldehyde (PF) resol for construction of ordered mesoporous framework. This new proof-of-concept synthetic methodology could greatly develop the self-assembly theories for the fabrication of well-defined porous polymer and carbon materials.

The reactive template is synthesized by transformation of the chain ends of the commercial triblock copolymer EO_{106}-PO_{70}-EO_{106} (F127) from hydroxymethyl group to aldehyde group (Supporting Information, Scheme S1). The aldehyde end-group of this reactive F127 (R-F127) can react with PF resol to form a stable covalent bond during the self-assembly process. In this way, the greatly enhanced interaction resulting from a magnificent combination of the covalent bond and the hydrogen bond between the PF resol and the R-F127 leads to a successful self-assembly for formation of an ordered body-centered cubic mesostructure, thus obtaining OMP after template removal and OMC after carbonization (Figure 1).

RESULTS AND DISCUSSION

As illustrated in Supporting Information, Scheme S1, oxidation of the hydroxymethyl end-group is carried out by treating triblock copolymer F127 with a mixture of acetic anhydride and dimethyl sulfoxide. The validity of this oxidation reaction can be obviously supported by the Fourier-transform infrared (FTIR) spectrum and proton nuclear magnetic resonance (^{1}H NMR) spectrum. After the oxidation reaction, a new peak at 9.59 ppm resulting from the −CHO group appears in the ^{1}H NMR spectrum of the R-F127 (Figure 2A and Supporting Information, Figure S1),[38] and the characteristic of absorption peak of the −CHO group is observed at 1734 cm^{-1} in the FTIR spectrum (Figure 2B and Supporting Information, Figure S2).[39,40] These results clearly demonstrate the successful formation of targeted reactive F127.

The as-prepared R-F127 is employed as the reactive template for cooperative self-assembly with PF resol in an aqueous solution. The resulting OMP sample shows three well-resolved diffraction peaks with a *d* spacing ratio of $1/(1/\sqrt{2})/(1/\sqrt{3})$ in its low-angle X-ray diffraction (XRD) patterns, which can be indexed as 110, 200, and 211 diffractions of a highly ordered body-centered cubic mesostructure (Figure 3).[37] These three peaks still exist in the XRD pattern of the resulting OMC, indicating that the ordered mesostructure is thermally stable (Figure 3). The unit cell parameter (*a*) of OMP and OMC are calculated to be 14.5 and 11.7 nm (Table 1), respectively, which reflects a slight shrinkage after carbonization. For comparison, a control polymer sample is prepared using the unreactive F127 as the template. As shown in Figure 3, the control sample does not display any diffraction peaks in the XRD pattern, indicative of the absence of mesostructure regularity. This is probably due to the weak interaction between F127 and PF resol. Such a comparison further confirms that the reactive nature of R-F127 plays a crucial role in the cooperative assembly of ordered mesostructure.

Transmission electron microscopy (TEM) images of the OMP, OMC, and control polymer sample are shown in Figure 4. OMP reveals a typical body-centered cubic mesostructure[37] that contains well-distributed ordered mesopores arising from the thermo-decomposition of hydrophobic PPO segment of R-F127. After a carbonization process, the ordered mesopore structure can still be observed in the TEM image of the resulting OMC (Figure 4B). In contrast, the TEM characterization

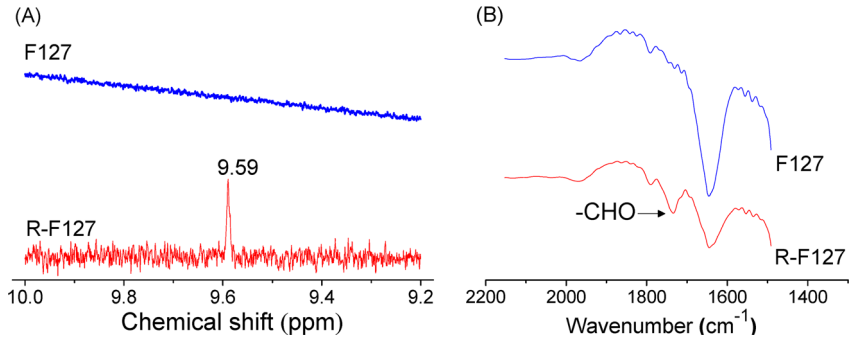

Figure 2. (A) ^{1}H NMR spectrum and (B) FTIR spectrum of triblock copolymer R-F127 and F127.

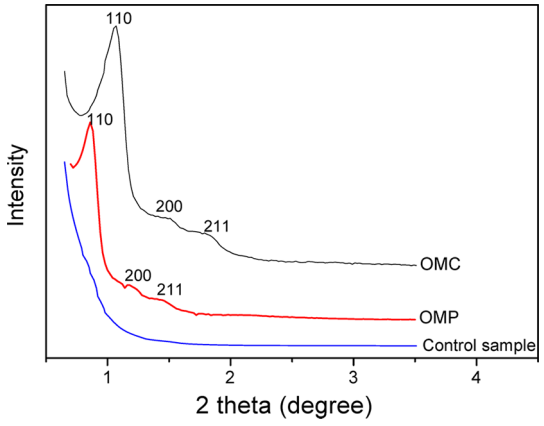

Figure 3. XRD patterns of typical samples.

of the control polymer sample shows a very poor and disordered pore framework. These findings are in good agreement with the XRD data shown in Figure 3. Taking the above results together, it is clearly demonstrated that the employment of the reactive template R-F127 is the key to formation of an ordered mesostructure. Generally, a periodic polymeric mesostructure can be formed only if there exists a strong enough interaction between building blocks (*e.g.*, polymer precursor) and organic templates (*e.g.*, triblock copolymer). However, at present, the organic templates generally interact with the building blocks just through noncovalent interactions such as hydrogen bonding, van der Waals forces, and electrostatic interaction.[41,42] Such kinds of interaction are too weak to act as a driving force for the formation of ordered mesostructures under many cooperative self-assembly conditions. For example, hydrogen-bonding interaction between the hydrophilic PEO segments of the unreactive F127 and hydroxyl groups of PF resol is not large enough for the ordered assembly, resulting in a disordered mesostructure. When using the reactive template R-F127, the aldehyde end-group of R-F127 can react with PF resol to form a stable covalent bond during the aqueous self-assemble process. Such an additional but necessary covalent bond greatly enhances the interaction between PF resol and the template and thus allows for a successful self-assembly for an ordered mesostructure.

The pore structure of the as-prepared samples is quantitatively analyzed by measurement of N_2 adsorption at 77 K (Figure 5). Both OMP and OMC show a type IV adsorption isotherm, indicative of a uniform mesopore structure.[37] It should be noted that the adsorption and desorption branches in the isotherm of OMP are not closed at the low relative pressure, which may be related to the activated adsorption effect, swelling effect, or limited access of nitrogen molecules to the pores.[43] The diameters of mesopore are calculated to be 5.0 nm for OMP and 3.2 nm for OMC with density functional theory (DFT) (see the inset in Figure 5). On the other hand, the adsorption amount of OMP increases very sharply at low relative pressure, indicating the existence of numerous micropores.[44] These micropores mainly center at 1.3 nm. After carbonization, numerous new micropores of 0.5 nm diameter are generated within the resulting carbon framework of OMC probably due to burnoff of many noncarbon elements and carbon-containing compounds during pyrolysis (see the inset Figure 5), which is similar to the case of OMCs obtained by conventional self-assembly procedures.[32,45] As a result, OMP and OMC exhibit high surface areas (311−637 m^2/g) and large pore volumes (0.25−0.32 cm^3/g), as shown in Table 1.

The porous polymer and carbon materials with highly ordered mesopore arrangement developed by the reactive template-induced self-assembly method can show potential for use in many applications. Here, the electrochemical capacitive performance of OMC is evaluated. As shown in Supporting Information, Figure S3, the cyclic voltammogram of OMC exhibits a rectangular-shaped pattern, implying a typical near-ideal capacitor behavior. For comparison, a commercial activated carbon YP-50 with BET surface area of 1417 m^2/g used for supercapacitors is also investigated under the same experimental conditions. It is found that OMC possesses superior specific capacitance to YP-50, no matter whether the sweep rate is high or low (Supporting Information, Figure S4). For example, at the sweep rate of 10 mV/s, the specific capacitance of OMC is 159 F/g, higher than 145 F/g for YP-50. This difference becomes more prominent with increasing sweep rates, indicating an excellent rate performance for OMC. Therefore,

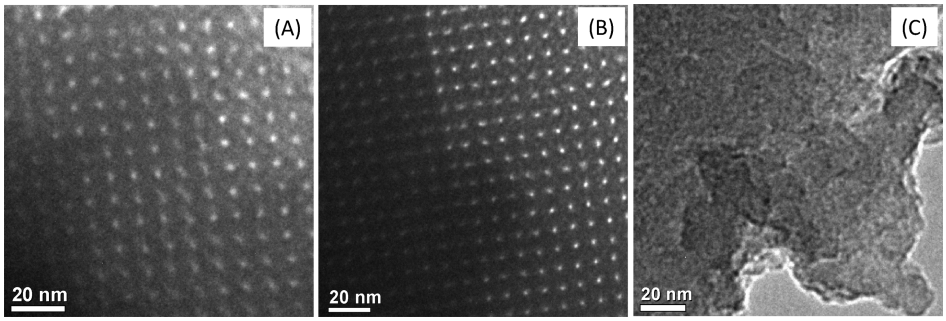

Figure 4. Typical TEM images of (A) OMP, (B) OMC, and (C) the control sample.

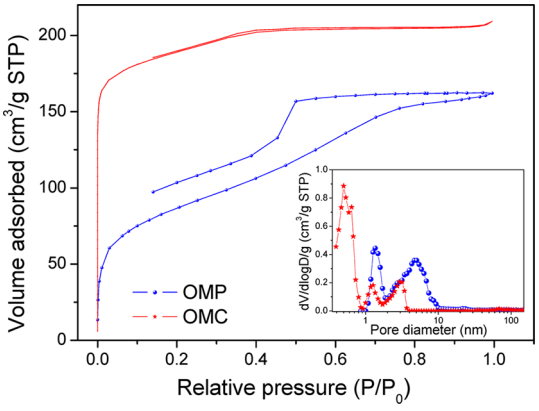

Figure 5. N_2 adsorption−desorption isotherms of OMP and OMC. The inset shows their DFT pore size distributions.

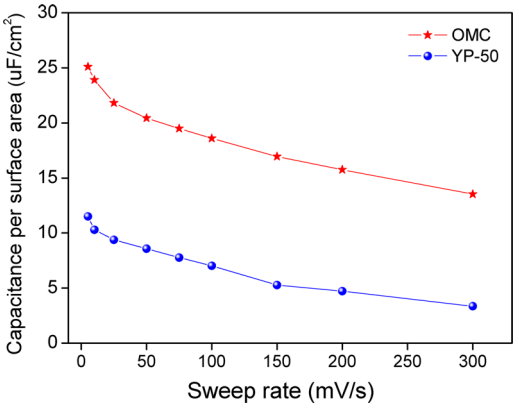

Figure 6. Capacitance per surface area of OMC and YP-50 at various sweep rates.

TABLE 1. Nanostructure Parameters of OMP and OMC[a]

sample	a (nm)	S_{BET} (m^2/g)	V_t (cm^3/g)	V_{mes} (cm^3/g)	V_{mic} (cm^3/g)
OMP	14.5	311	0.25	0.31	0.02
OMC	11.7	637	0.32	0.15	0.21

[a] a, S_{BET}, V_t, V_{mes} and V_{mic} are the unit cell parameter, BET surface area, total pore volume, mesopore volume obtained by BJH method, and micropore volume obtained by *t*-plot method, respectively.

OMC shows a higher capacitance retention ratio as compared to YP-50, especially at the high sweep rates (Supporting Information, Figure S5). The significant superiority of OMC over YP-50 in terms of the electrochemical performances could be attributed to its more advanced porous structure. As an activated carbon, YP-50 contains a large proportion of disordered mircropores (Supporting Information, Figure S6), most of which are located in the micrometer/millimeter-scaled carbon particles.[46] Many of its inner micropores are difficult to immerse by electrolyte because of the absence of enough transport pathways for the ion diffusion, leading to a poor utilization of the surface area. For OMC, its mesopores are well-distributed in a regular pattern, which is very favorable for access of ions, and provide fast ion transport pathways to the micropores within the well-arranged carbon framework of *ca.* 7 nm thickness, greatly enhancing the utilization of the pore surface. As shown in Figure 6, the specific capacitance per surface area for OMC far exceeds that of YP-50 at all sweep rates, suggesting that the surface of nanopores for OMC is much more electrochemically active than that for YP-50. Particularly, the specific capacitance per surface area of OMC obtained at 5 mV/s is 25.1 μF/cm^2, a value higher than those of many other typical carbon materials including conventional porous carbons,[47−50] OMC with hexagonal mesostructure,[25] OMC with body-centered cubic mesostructure,[51] and modified graphene[52] in aqueous electrolytes (7−21 μF/cm^2). These superior capacitive behaviors, including large capacitance, excellent rate capability, and extraordinarily efficient electrochemically active surface area, may provide OMC with great potential for use as high performance supercapacitor electrodes.

CONCLUSIONS

A novel synthetic methodology based on the reactive template-induced self-assembly has been successfully developed to prepare ordered mesoporous polymeric and carbonaceous materials. The aldehyde group at the chain end of reactive template R-F127 can react with PF resol to *in-situ* form a stable covalent bond during the self-assembly process. With the employment of this reactive template for enhancing the interaction between PF resol and triblock copolymer,

a highly ordered body-centered cubic mesostructure can be formed. Such an ordered mesostructure can be directly transformed into ordered mesoporous polymer after template removal and ordered mesoporous carbon after carbonization. The ordered mesoporous carbon demonstrates better capacitive performance than the commercial activated carbon for supercapacitor, presenting an attractive potential candidate for high performance supercapacitor electrodes. These as-prepared ordered mesoporous materials could find utility in many other applications like fuel cell, catalysis, and adsorption toward volatile organic compounds. We hope that this new concept of reactive template-induced self-assembly would promote the progress of fabrication science for mesoporous polymer and carbon materials.

METHODS

Preparation of the Reactive Template R-F127. The reactive template R-F127 containing the aldehyde end-group was synthesized by oxidization of the triblock copolymer F127 with the mixture of acetic anhydride (Ac_2O) and dimethyl sulfoxide (DMSO). A 2.5 g portion of F127 was immersed in 10 mL of DMSO in a conical flask. Subsequently, 0.5 mL of Ac_2O was added to the mixture to achieve a final Ac_2O/−OH molar ratio of about 20:1. The reaction was allowed to proceed for about 8 h at room temperature under stirring. The resulting polymer sample was precipitated in 8 volumes of diethyl ether. After that, the polymer was redissolved in minimum methylene chloride and precipitated again in 8 volumes of diethyl ether. The above precipitation−dissolution procedure was repeated four times. The polymer was finally dried overnight under vacuum, leading to the R-F127.

Preparation of Ordered Mesoporous Materials. According to the molar ratio of phenol/formaldehyde/NaOH/R-F127 = 1.0/3.5/0.24/0.0075, 1.0 g of phenol and 2.8 mL of 40 wt % formaldehyde were dissolved in 25 mL of 0.1 M NaOH solution, and then a clear phenol-formaldehyde resol was obtained after stirring at 68 °C for 30 min. Subsequently, 1 g of R-F127 was completely dissolved in 25 mL of water, followed by the addition of the as-made resol solution. The mixture was continuously stirred at 65 °C for 96 h and then stirred at 70 °C for another 24 h. The product was collected, washed with water, and dried at 100 °C in air. After that, the as-made sample was calcined under N_2 flow at 350 °C for 3 h to obtain the OMP, and at 800 °C for 3 h to obtain the OMC. The heating rate was 1 °C/min below 600 °C and increased to 5 °C/min above 600 °C. For comparison, a control sample was synthesized. Its preparation procedure was exactly the same as that of the OMP except that the unreactive F127 was employed as the organic template.

Structure Characterization. Low-angle XRD patterns were recorded on a D-MAX 2200 VPC diffractometer using Cu Kα radiation (40 kV, 30 mA). The unit cell parameter (a) was calculated using the formula $a = (\sqrt{2})d_{110}$, where d_{110} represents the d-spacing value of the 110 diffraction. TEM images were obtained by a JEM-2010HR microscope. The FTIR measurements of the samples were performed with IR spectroscopy (Bruker TENSOR 27), using the KBr disk method. ^{1}H NMR was measured on a Mercury-Plus 300 spectrometer. N_2 adsorption measurements were carried out using a Micromeritics ASAP 2010 analyzer at 77 K. The BET surface area (S_{BET}) and the mesopore volume (V_{mes}) were determined by Brunauer−Emmett−Teller (BET) theory and Barrett−Joyner−Halendar (BJH) method, respectively. The total pore volume (V_t) was estimated from the amount adsorbed at a relative pressure P/P_0 of 0.990. The micropore volume (V_{mic}) was determined by t-plot theory. The pore size distribution was analyzed by original density functional theory (DFT) combined with non-negative regularization and medium smoothing. The framework thickness (t) was calculated using the formula $t = (\sqrt{3})a/2 - D$,[32] where a and D are the unit cell parameter and the DFT mesopore diameter, respectively.

Electrochemical Measurement. The carbon electrodes in the form of a round sheet were obtained by pressing a mixture film of 92 wt % carbon sample and 8 wt % polytetrafluorethylene into a nickel foam current collector. Cyclic voltammetry measurement was carried out using an IM6e electrochemical workstation with a typical three-electrode configuration in 6 M KOH aqueous solution. Hg/HgO was chosen as a reference electrode. The specific capacitance (C_m) was calculated according to the equation $C_m = I/(\nu m)$, where I, ν, and m represent the current at the middle voltage of the potential window, the sweep rate, and the mass of the carbon sample, respectively. The capacitance per surface area (C_s) was calculated according to the equation $C_s = C_m/S_{BET}$, where S_{BET} is the BET surface area.

Conflict of Interest: The authors declare no competing financial interest.

Acknowledgment. We acknowledge financial support from the project of NSFC (51173213, 51172290, 50802116, 51232005), Program for New Century Excellent Talents in University, Program for Pearl River New Star of Science and Technology in Guangzhou, the Fundamental Research Funds for the Central Universities (09lgpy18), and the Project of Demonstration Base of Department of Education of Guangdong Province (cgzhzd0901). The authors also would like to thank Mr. Bin Sun for his help in drawing the schematic diagram.

Supporting Information Available: Synthetic route to R-F127, ^{1}H NMR spectrum, FTIR spectrum, cyclic voltammogram, mass specific capacitance, capacitance retention ratio, and pore size distribution. This material is available free of charge *via* the Internet at http://pubs.acs.org.

REFERENCES AND NOTES

1. Wu, D.; Xu, F.; Sun, B.; Fu, R.; He, H.; Matyjaszewski, K. Design and Preparation of Porous Polymers. *Chem. Rev.* **2012**, *112*, 3959–4015.
2. Wang, D. W.; Li, F.; Liu, M.; Lu, G. Q.; Cheng, H. M. 3D Aperiodic Hierarchical Porous Graphitic Carbon Material for High-Rate Electrochemical Capacitive Energy Storage. *Angew. Chem., Int. Ed.* **2008**, *47*, 373–376.
3. Davis, M. E. Ordered Porous Materials for Emerging Applications. *Nature* **2002**, *417*, 813–821.
4. Liang, Y.; Feng, X.; Zhi, L.; Kolb, U.; Muellen, K. A Simple Approach Towards One-Dimensional Mesoporous Carbon with Superior Electrochemical Capacitive Activity. *Chem. Commun.* **2009**, 809–811.
5. Su, D. S.; Schlogl, R. Nanostructured Carbon and Carbon Nanocomposites for Electrochemical Energy Storage Applications. *ChemSusChem* **2010**, *3*, 136–168.
6. Fan, Z.; Liu, Y.; Yan, J.; Ning, G.; Wang, Q.; Wei, T.; Zhi, L.; Wei, F. Template-Directed Synthesis of Pillared-Porous Carbon Nanosheet Architectures: High-Performance Electrode Materials for Supercapacitors. *Adv. Energy Mater.* **2012**, *2*, 419–424.
7. Wu, D.; Nese, A.; Pietrasik, J.; Liang, Y.; He, H.; Kruk, M.; Huang, L.; Kowalewski, T.; Matyjaszewski, K. Preparation of Polymeric Nanoscale Networks from Cylindrical Molecular Bottlebrushes. *ACS Nano* **2012**, *6*, 6208–6214.
8. Peng, H.; Sun, X. Macroporous Carbon Nanotube Arrays with Tunable Pore Sizes and Their Template Applications. *Chem. Commun.* **2009**, 1058–1060.
9. Nishihara, H.; Yang, Q. H.; Hou, P.-X.; Unno, M.; Yamauchi, S.; Saito, R.; Paredes, J. I.; Martínez-Alonso, A.; Tascón, J. M. D.; Sato, Y.; *et al.* A Possible Buckybowl-like Structure of Zeolite Templated Carbon. *Carbon* **2009**, *47*, 1220–1230.

10. Chen, C. M.; Zhang, Q.; Huang, J. Q.; Zhang, W.; Zhao, X. C.; Huang, C. H.; Wei, F.; Yang, Y. G.; Wang, M. Z.; Su, D. S. Chemically Derived Graphene–Metal Oxide Hybrids as Electrodes for Electrochemical Energy Storage: Pre-graphenization or Post-graphenization?. *J. Mater. Chem.* **2012**, *22*, 13947–13955.
11. Qiao, Y.; Wang, D.; Buriak, J. M. Block Copolymer Templated Etching on Silicon. *Nano Lett.* **2007**, *7*, 464–469.
12. Saghatelian, A.; Buriak, J.; Lin, V. S. Y.; Ghadiri, M. R. Transition Metal Mediated Surface Modification of Porous Silicon. *Tetrahedron* **2001**, *57*, 5131–5136.
13. Liang, Y.; Schwab, M. G.; Zhi, L.; Mugnaioli, E.; Kolb, U.; Feng, X.; Muellen, K. Direct Access to Metal or Metal Oxide Nanocrystals Integrated with One-Dimensional Nanoporous Carbons for Electrochemical Energy Storage. *J. Am. Chem. Soc.* **2010**, *132*, 15030–15037.
14. Ding, X. S.; Guo, J.; Feng, X. A.; Honsho, Y.; Guo, J. D.; Seki, S.; Maitarad, P.; Saeki, A.; Nagase, S.; Jiang, D. L. Synthesis of Metallophthalocyanine Covalent Organic Frameworks that Exhibit High Carrier Mobility and Photoconductivity. *Angew. Chem., Int. Ed.* **2011**, *50*, 1289–1293.
15. Choi, M.; Ryoo, R. Ordered Nanoporous Polymer-Carbon Composites. *Nat. Mater.* **2003**, *2*, 473–476.
16. Zalusky, A. S.; Olayo-Valles, R.; Wolf, J. H.; Hillmyer, M. A. Ordered Nanoporous Polymers from Polystyrene–Polylactide Block Copolymers. *J. Am. Chem. Soc.* **2002**, *124*, 12761–12773.
17. Jun, S.; Joo, S. H.; Ryoo, R.; Kruk, M.; Jaroniec, M.; Liu, Z.; Ohsuna, T.; Terasaki, O. Synthesis of New, Nanoporous Carbon with Hexagonally Ordered Mesostructure. *J. Am. Chem. Soc.* **2000**, *122*, 10712–10713.
18. Zhao, X. C.; Zhang, Q.; Zhang, B. S.; Chen, C. M.; Wang, A. Q.; Zhang, T.; Su, D. S. Dual-Heteroatom-Modified Ordered Mesoporous Carbon: Hydrothermal Functionalization, Structure, and Its Electrochemical Performance. *J. Mater. Chem.* **2012**, *22*, 4963–4969.
19. Lee, J.; Kim, J.; Hyeon, T. Recent Progress in the Synthesis of Porous Carbon Materials. *Adv. Mater.* **2006**, *18*, 2073–2094.
20. Peng, H. S.; Tang, J.; Yang, L.; Pang, J. B.; Ashbaugh, H. S.; Brinker, C. J.; Yang, Z. Z.; Lu, Y. F. Responsive Periodic Mesoporous Polydiacetylene/Silica Nanocomposites. *J. Am. Chem. Soc.* **2006**, *128*, 5304–5305.
21. Ding, X. S.; Feng, X.; Saeki, A.; Seki, S.; Nagai, A.; Jiang, D. L. Conducting Metallophthalocyanine 2D Covalent Organic Frameworks: The Role of Central Metals in Controlling π-Electronic Functions. *Chem. Commun.* **2012**, *48*, 8952–8954.
22. Nagai, A.; Guo, Z.; Feng, X.; Jin, S.; Chen, X.; Ding, X.; Jiang, D. Pore Surface Engineering in Covalent Organic Frameworks. *Nat. Commun.* **2011**, *2*, 536–544.
23. Liang, C. D.; Li, Z. J.; Dai, S. Mesoporous Carbon Materials: Synthesis and Modification. *Angew. Chem., Int. Ed.* **2008**, *47*, 3696–3717.
24. Su, D. S.; Delgado, J. J.; Liu, X.; Wang, D.; Schloegl, R.; Wang, L.; Zhang, Z.; Shan, Z.; Xiao, F.-S. Highly Ordered Mesoporous Carbon as Catalyst for Oxidative Dehydrogenation of Ethylbenzene to Styrene. *Chem. Asian J.* **2009**, *4*, 1108–1113.
25. Liang, Y.; Wu, D.; Fu, R. Preparation and Electrochemical Performance of Novel Ordered Mesoporous Carbon with an Interconnected Channel Structure. *Langmuir* **2009**, *25*, 7783–7785.
26. Munoz, B.; Ramila, A.; Perez-Pariente, J.; Diaz, I.; Vallet-Regi, M. MCM-41 Organic Modification as Drug Delivery Rate Regulator. *Chem. Mater.* **2003**, *15*, 500–503.
27. Wu, Z. X.; Zhao, D. Y. Ordered Mesoporous Materials as Adsorbents. *Chem. Commun.* **2011**, *47*, 3332–3338.
28. Liu, R. L.; Wu, D. Q.; Feng, X. L.; Mullen, K. Nitrogen-Doped Ordered Mesoporous Graphitic Arrays with High Electrocatalytic Activity for Oxygen Reduction. *Angew. Chem., Int. Ed.* **2010**, *49*, 2565–2569.
29. Wang, D. W.; Li, F.; Chen, Z.-G.; Lu, G. Q.; Cheng, H. M. Synthesis and Electrochemical Property of Boron-Doped Mesoporous Carbon in Supercapacitor. *Chem. Mater.* **2008**, *20*, 7195–7200.
30. Wang, D. W.; Li, F.; Fang, H. T.; Liu, M.; Lu, G. Q.; Cheng, H. M. Effect of Pore Packing Defects in 2-D Ordered Mesoporous Carbons on Ionic Transport. *J. Phys. Chem. B* **2006**, *110*, 8570–8575.
31. Zhai, Y.; Dou, Y.; Zhao, D.; Fulvio, P. F.; Mayes, R. T.; Dai, S. Carbon Materials for Chemical Capacitive Energy Storage. *Adv. Mater.* **2011**, *23*, 4828–4850.
32. Zhang, F.; Meng, Y.; Gu, D.; Yan, Y.; Chen, Z.; Tu, B.; Zhao, D. An Aqueous Cooperative Assembly Route to Synthesize Ordered Mesoporous Carbons with Controlled Structures and Morphology. *Chem. Mater.* **2006**, *18*, 5279–5288.
33. Tanaka, S.; Nishiyama, N.; Egashira, Y.; Ueyama, K. Synthesis of Ordered Mesoporous Carbons with Channel Structure from an Organic–Organic Nanocomposite. *Chem. Commun.* **2005**, 2125–2127.
34. Liang, C. D.; Hong, K. L.; Guiochon, G. A.; Mays, J. W.; Dai, S. Synthesis of a Large-Scale Highly Ordered Porous Carbon Film by Self-Assembly of Block Copolymers. *Angew. Chem., Int. Ed.* **2004**, *43*, 5785–5789.
35. Wan, Y.; Shi, Y. F.; Zhao, D. Y. Supramolecular Aggregates as Templates: Ordered Mesoporous Polymers and Carbons. *Chem. Mater.* **2008**, *20*, 932–945.
36. Fang, Y.; Gu, D.; Zou, Y.; Wu, Z.; Li, F.; Che, R.; Deng, Y.; Tu, B.; Zhao, D. A Low-Concentration Hydrothermal Synthesis of Biocompatible Ordered Mesoporous Carbon Nanospheres with Tunable and Uniform Size. *Angew. Chem., Int. Ed.* **2010**, *49*, 7987–7991.
37. Meng, Y.; Gu, D.; Zhang, F.; Shi, Y.; Cheng, L.; Feng, D.; Wu, Z.; Chen, Z.; Wan, Y.; Stein, A.; *et al*. A Family of Highly Ordered Mesoporous Polymer Resin and Carbon Structures from Organic–Organic Self-Assembly. *Chem. Mater.* **2006**, *18*, 4447–4464.
38. Rathna, G. V. N. Hydrogels of Modified Ethylenediaminetetraacetic Dianhydride Gelatin Conjugated with Poly(ethylene glycol) Dialdehyde as a Drug-Release Matrix. *J. Appl. Polym. Sci.* **2004**, *91*, 1059–1067.
39. Li, Y. L.; Neoh, K. G.; Kang, E. T. Poly(vinyl alcohol) Hydrogel Fixation on Poly(ethylene terephthalate) Surface for Biomedical Application. *Polymer* **2004**, *45*, 8779–8789.
40. Llanos, G. R.; Sefton, M. V. Immobilization of Poly(ethylene glycol) onto a Poly(vinyl alcohol) Hydrogel. 1. Synthesis and Characterization. *Macromolecules* **1991**, *24*, 6065–6072.
41. Yang, Z. L.; Lu, Y. F.; Yang, Z. Z. Mesoporous Materials: Tunable Structure, Morphology and Composition. *Chem. Commun.* **2009**, 2270–2277.
42. Brinker, C. J.; Lu, Y. F.; Sellinger, A.; Fan, H. Y. Evaporation-Induced Self-Assembly: Nanostructures Made Easy. *Adv. Mater.* **1999**, *11*, 579–585.
43. Rose, M.; Bohlmann, W.; Sabo, M.; Kaskel, S. Element-Organic Frameworks with High Permanent Porosity. *Chem. Commun.* **2008**, *0*, 2462–2464.
44. Wu, D.; Hui, C. M.; Dong, H.; Pietrasik, J.; Ryu, H. J.; Li, Z.; Zhong, M.; He, H.; Kim, E. K.; Jaroniec, M.; *et al*. Nanoporous Polystyrene and Carbon Materials with Core–Shell Nanosphere-Interconnected Network Structure. *Macromolecules* **2011**, *44*, 5846–5849.
45. Wang, X.; Liang, C.; Dai, S. Facile Synthesis of Ordered Mesoporous Carbons with High Thermal Stability by Self-Assembly of Resorcinol-Formaldehyde and Block Copolymers under Highly Acidic Conditions. *Langmuir* **2008**, *24*, 7500–7505.
46. Xu, F.; Cai, R.; Zeng, Q.; Zou, C.; Wu, D.; Li, F.; Lu, X.; Liang, Y.; Fu, R. Fast Ion Transport and High Capacitance of Polystyrene-Based Hierarchical Porous Carbon Electrode Material for Supercapacitors. *J. Mater. Chem.* **2011**, *21*, 1970–1976.
47. Frackowiak, E. Carbon Materials for Supercapacitor Application. *Phys. Chem. Chem. Phys.* **2007**, *9*, 1774–1785.
48. Frackowiak, E.; Béguin, F. Carbon Materials for the Electrochemical Storage of Energy in Capacitors. *Carbon* **2001**, *39*, 937–950.
49. Liang, Y. R.; Liang, F. X.; Li, Z. H.; Wu, D. C.; Yan, F. Y.; Li, S. Y.; Fu, R. W. The Role of Mass Transport Pathway in Wormhole-like Mesoporous Carbon for Supercapacitors. *Phys. Chem. Chem. Phys.* **2010**, *12*, 10842–10845.

50. Zhong, M.; Kim, E. K.; McGann, J. P.; Chun, S.-E.; Whitacre, J. F.; Jaroniec, M.; Matyjaszewski, K.; Kowalewski, T. Electrochemically Active Nitrogen-Enriched Nanocarbons with Well-Defined Morphology Synthesized by Pyrolysis of Self-Assembled Block Copolymer. *J. Am. Chem. Soc.* **2012**, *134*, 14846–14857.
51. Sun, G. W.; Wang, J. T.; Liu, X. J.; Long, D. H.; Qiao, W. M.; Ling, L. C. Ion Transport Behavior in Triblock Copolymer-Templated Ordered Mesoporous Carbons with Different Pore Symmetries. *J. Phys. Chem. C* **2010**, *114*, 18745–18751.
52. Stoller, M. D.; Park, S. J.; Zhu, Y. W.; An, J. H.; Ruoff, R. S. Graphene-Based Ultracapacitors. *Nano Lett.* **2008**, *8*, 3498–3502.